

INCORPORATION OF DIPYRIDAMOLE INTO HYDROXYAPATITE FOR BONE GRAFT APPLICATION

Georgia Dutra Soares Brandão Martins, Instituto Militar de Engenharia - IME, georgia.martins@ime.eb.br, <https://orcid.org/0009-0001-0622-4617>. **Ary Machado de Azevedo**, Instituto Militar de Engenharia – IME, ary@ime.eb.br, <https://orcid.org/0009-0007-6517-8423>. **Marcelo Henrique Prado da Silva**, Instituto Militar de Engenharia – IME, marceloprado@ime.eb.br, <https://orcid.org/0000-0002-1182-5345>. **André Aguiar Marques**, Instituto Militar de Engenharia - IME, andre.marques@ime.eb.br, <https://orcid.org/0000-0003-1511-4038>. **Álvaro José Boareto Mendes**, Instituto Militar de Engenharia – IME, boaretomendes@yahoo.com.br, <https://orcid.org/0000-0003-1432-9045>. **Carlos Nelson Elias**, Instituto Militar de Engenharia – IME, elias@ime.eb.br, ORCID <https://orcid.org/0000-0002-7560-6926>

DOI:

ABSTRACT

Hydroxyapatite (HAp) is widely used in bone tissue engineering and bone grafting due to its bioactivity and resorption potential. The incorporation of bioactive molecules, such as dipyridamole (DIPY), may enhance its osteoinductive potential. This study investigates the influence of DIPY incorporation into HA and evaluates the physicochemical interactions using scanning electron microscopy (SEM) and energy-dispersive X-ray spectroscopy (EDS). HAp was synthesized via wet precipitation, and the specimens were treated with DIPY solutions (100 μ M and 1,000 μ M) prepared in absolute ethanol and methanol, as well as in 70% solutions. All groups were dried at room temperature. FTIR analysis was employed to identify characteristic DIPY bands and to detect potential solvent residues. Spectral comparisons among the groups enabled interpretation of incorporation efficiency and interactions with the ceramic matrix. The results support the development of drug-functionalized bioceramics for bone repair applications.

Keywords: bone grafts, bone substitutes, biomaterials, biocompatibility.

1 Introduction

Bone regeneration remains a major challenge in dentistry and orthopedics, particularly in cases involving bone defects where the body's natural regenerative capacity is limited. The use of biomaterials has become a key strategy to overcome this limitation, with hydroxyapatite (HA) being one of the most widely used materials due to its chemical similarity to the natural bone matrix, osteoconductive properties, high biocompatibility, and excellent integration into bone tissue (Dorozhkin et al., 2010; LeGeros et al., 2008).

Despite these advantages, hydroxyapatite has a low osteoinductive capacity, meaning it does not directly stimulate osteogenic cell differentiation, which may limit its effectiveness in low-regeneration environments. To address this drawback, biofunctionalization strategies have been investigated to enhance cellular responses and promote bone formation (Rezwan et al., 2006).

Among the compounds studied, dipyridamole stands out as a pharmacological agent traditionally used as a vasodilator and antiplatelet drug, which has also demonstrated osteogenic potential in recent studies. Evidence suggests that dipyridamole modulates cellular signaling pathways, promoting osteoblastic differentiation and extracellular matrix mineralization (Ali et al., 2019; Yao et al., 2020).

Based on this rationale, the present study proposes incorporating dipyridamole into hydroxyapatite. For this purpose, XRD tests were carried out to verify the phases present, SEM was used to assess morphology, and EDS was used to determine the chemical composition.

2 Materials and Methods

The method used to obtain hydroxyapatite (HAp) involved precipitation in an aqueous medium (Silveira, P.H.P.M. et al., 2024). An aqueous solution containing 0.5 M suspended calcium hydroxide (Merck, Darmstadt, Germany) and 1 M lactic acid (Vetec, Rio de Janeiro, Brazil) was stirred magnetically for 30 minutes. Subsequently, a 0.3 M solution of orthophosphoric acid (Merck, Darmstadt, Germany) was slowly dripped (8 ml/min) into the prepared solution. After 60 min of magnetic stirring, a 1.2 M sodium hydroxide solution (Merck, Darmstadt, Germany) was added, raising the pH to 12 and precipitating hydroxyapatite. Twenty-four hours later, the precipitate was filtered under vacuum and washed with deionized water until the final pH reached 7. For sample preparation, the precipitate was dried at 80°C for 24h and subsequently de-agglomerated in a ceramic mortar. The obtained powder was subjected to uniaxial pressing at 1.0 ton, resulting in discs weighing 0.150g, with a diameter of 6 mm and a height of 2.5 mm.

Subsequently, solutions of 70% ethanol and 70% methanol were prepared, as well as pure ethanol and pure methanol solutions. In addition, the drug dipyridamole (DIPY), analytical grade, supplied by Start BioScience with a purity level of 99.29%, was incorporated into these solutions.

To determine the effect of the DIPY solution on HAp, it is necessary to compare the results obtained with different alcohols. To this end, four solvent groups were created: analytical-grade ethanol, analytical-grade methanol, 70% ethanol, and 70% methanol. Figure 1 illustrates the grouping of these conditions.

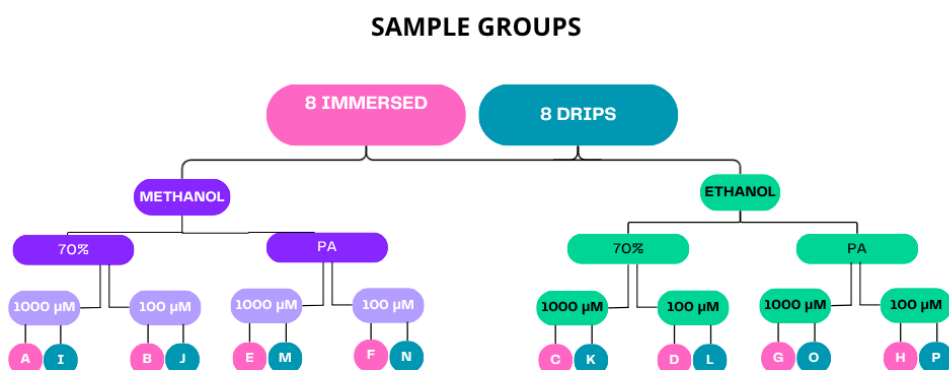


Figure 1. A sample group.

Samples from the first group were immersed in the solution. Samples A and B were prepared using 70% methanol at concentrations of 1000 μM and 100 μM , respectively. Samples C and D followed the same concentration scheme but were prepared using 70% ethanol, a second group. Similarly, samples E and F were prepared with methanol PA, while samples G and H were prepared with ethanol PA, both following the same two concentrations.

The third group is a controlled droplet method. Samples I and J were prepared using 70% methanol at concentrations of 1000 μM and 100 μM , respectively. Samples K and L were prepared in 70% ethanol at 1000 μM and 100 μM , respectively. Samples M and N were prepared with methanol PA, and samples O and P with ethanol PA, maintaining the same concentration levels in a fourth group.

After incorporation, the samples were subjected to different characterization analyses. Initially, a Structural Integrity in Solution test was performed to evaluate the physical stability of the tablets in a liquid medium. Subsequently, morphological analyses were carried out using Scanning Electron Microscopy (SEM), and chemical analyses were performed using Energy-Dispersive X-ray Spectroscopy (EDS), a non-destructive analytical technique used to identify and quantify the chemical elements present in a material. Furthermore, X-ray Diffraction (XRD) is a technique used to characterize crystalline materials and determine their phases.

2.1 Characterization

2.1.1 Structural Integrity Test in Solution

One of the tests performed was the deterioration assay, in which the samples, in disc form and unsintered, were immersed in 5 mL of each of the eight previously described solutions, all prepared with the DEEP vehicle. The immersions were carried out in 20 mL beakers, each designated for a specific solution, and properly sealed with a resistant plastic film to prevent evaporation or external contamination during the exposure period. The samples remained immersed for 17 hours.

2.1.2 Characterization by Scanning Electron Microscopy and Energy-Dispersive Spectroscopy

The morphology and elemental composition of the synthesized samples were observed using a FEG-SEM (Quanta 250FEG, FEI, Hillsboro, OR, USA) at the Military Institute of Engineering (IME), operating at 20 kV and equipped with an EDX detector. The samples for FEG-SEM examination were prepared by placing the samples on a conductive carbon tape and subsequently sputtering them with gold. The samples were previously cataloged and organized into groups based on the DIPY incorporation method (immersion or controlled droplet), with an alphabetical labeling system to ensure better control and organization during analysis.

The SEM analysis aimed to observe potential changes in the surface morphology of the samples resulting from variations in solvent type, DIPY concentration, and incorporation method. The EDS analysis, in turn, was conducted to determine the elemental composition of the samples, enabling the detection of elements indicative of DIPY incorporation into the material's matrix.

2.1.3 X-ray diffraction

X-ray diffraction (XRD) analyses were performed to identify and compare the crystalline phases of the samples, since each crystalline compound exhibits a characteristic peak pattern, a “fingerprint” that enables identification through comparison with databases such as the ICDD.

In this analysis, peak position (2θ), intensity, and width were evaluated; sharp, well-defined peaks were considered indicative of high crystallinity, whereas low-intensity halos or increased background noise were interpreted as evidence of amorphous material. DIPY is an amorphous material and therefore does not exhibit a crystalline structure.

3 Results

3.1 Structural Integrity Test in Solution

At the end of this period, the discs were removed and carefully examined. No visible physical alterations or signs of deterioration were observed. The samples maintained their structural integrity and did not release residues or show any evidence of disintegration in the liquid medium.

3.2 X-Ray Diffraction

Figure 2 shows the XRD patterns for all treatment groups and indicates preservation of the hydroxyapatite (HAp) crystalline phase, with no new diffraction peaks attributable to dipyrindamole (DIPY). Additionally, a new reflection appears at approximately $2\theta \approx 42^\circ$, which can be indexed to calcium oxide (CaO) (ICCD 01-072-1243), evidencing partial degradation of HAp; all other peaks were indexed to hydroxyapatite (ICCD 00-054-0022). Notably, this CaO peak is absent in Figure 3c, suggesting that exposure to ethanol or methanol, or the presence of DIPY during processing, may have contributed to the observed degradation in the other conditions. This interpretation is consistent with reports on DIPY-coated or DIPY-loaded bioceramic scaffolds, where DIPY enhances *in vivo* bone regeneration without introducing detectable crystalline changes in the ceramic matrix by XRD; the drug’s primary contribution stems from biological action via adenosine-receptor modulation rather than structural modification of the carrier (Ishack et al., 2015; Wang et al., 2019).

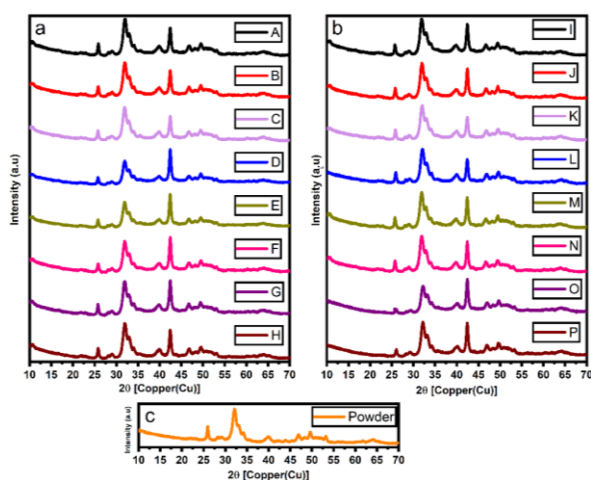


Figure 2. XRD Result: (a) Samples with ethanol; (b) Samples with methanol; (c) Powder of Hap.

However, to confirm the presence of DIPY, additional analyses are required, such as Fourier-transform infrared spectroscopy (FTIR) and Raman spectroscopy, as these techniques specifically assess chemical structure. Without these complementary assays, it is only possible to state that an amorphous material was introduced; it cannot be determined whether this material is DIPY or residual solvents, despite the volatility of the solvents used (National Institute of Standards and Technology, 2024; PubChem, 2024; Bozorgmehr et al., 2021, McGlashan et al., 1976, Kurihara et al., 1993, Dortmund Data Bank, 2024). Therefore, these additional tests are recommended before making definitive attributions.

3.3 Results of SEM Analysis

SEM analysis was performed to evaluate potential changes in surface morphology resulting from solvent type and concentration, as well as from the DIPY incorporation technique. The micrographs showed (Figure 3) that across all tested combinations. Thus, under the tested conditions, the DIPY incorporation process does not induce degradation or structural modifications observable by SEM.

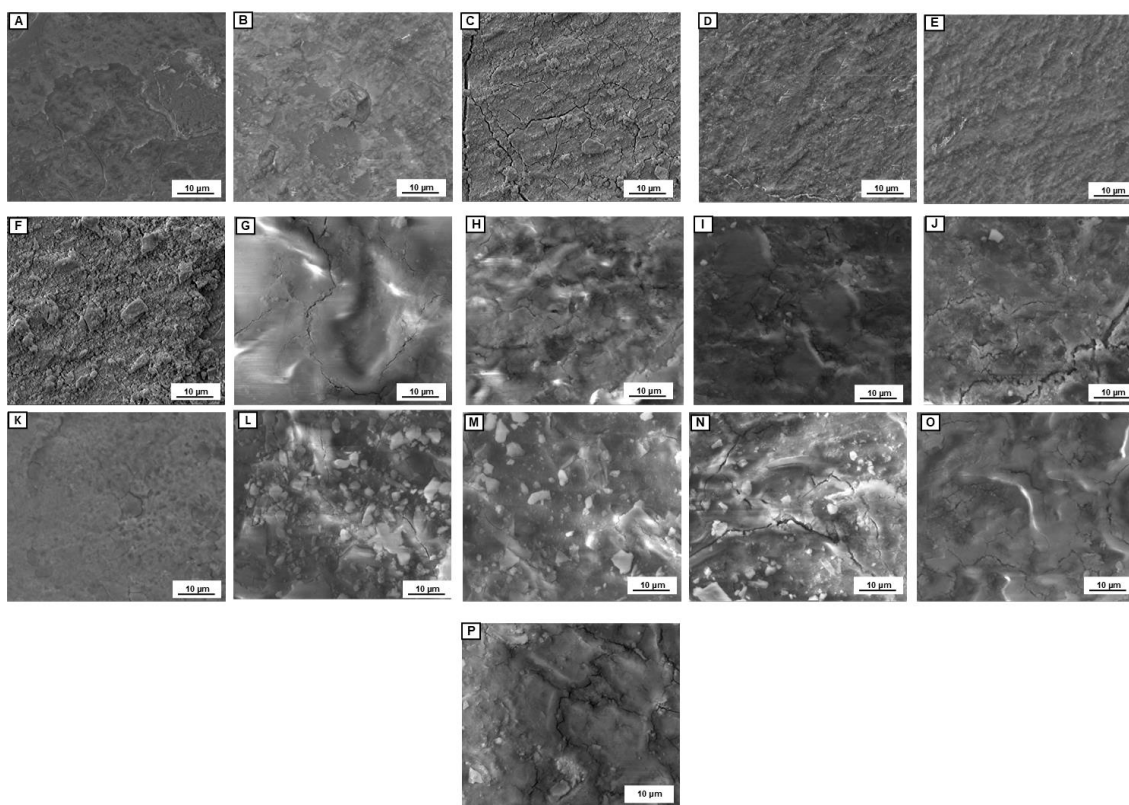


Figure 3. SEM images of all groups

EDS was used to determine the elemental composition of the samples and to probe for signatures of DIPY incorporation into the matrix. Table 1 summarizes the composition of each sample. The spectra showed carbon (C), oxygen (O), and calcium (Ca) as the predominant elements, consistent with hydroxyapatite and related structural constituents. No nitrogen (N) peaks were detected, which would have been a helpful indicator of DIPY, given the drug's nitrogen-containing groups.

Table 1. Sample`s chemical composition. EDS analysis.

Samples	C	O	P	Ca
A	6.73	49,02	16.57	27.68
B	6.11	42.10	19.39	32.39
C	5.33	30.83	23.91	39.93
D	5.04	34.72	22.56	37.68
E	9.37	51.52	14.65	24.46
F	11.45	49.96	14.45	24.13
G	12.53	55.08	12.13	20.26
H	11.67	57.67	11.48	19.17
I	13.11	58.48	10.64	17.77
J	12.71	55.65	11.85	19.79
K	11.32	42.56	17.27	28.85
L	9.07	58.79	12.04	20.10
M	7.44	56.01	13.69	22.86
N	9.57	36.71	20.12	33.60
O	8.32	51.89	14.90	24.89
P	7.58	55.53	13.82	23.07

The lack of a measurable N signal may reflect the low EDS sensitivity to light elements, a DIPY concentration below the detection limit, or superficial incorporation that is ineffective or non-homogeneous. A stoichiometric check gave $Ca/P \approx 1.67$, within the acceptable range for hydroxyapatite—and this is also supported by the XRD patterns, Figure 2, confirming phosphate–calcium conformity. Finally, the elevated C signal in EDS is attributable to sample preparation, as specimens were mounted on the stub with carbon tape.

3 DISCUSSION

The results of this study show the incorporation of dipyrnidamole (DIPY) into the hydroxyapatite (HA) matrix. In the XRD test, a phase transformation from HAp to calcium oxide (CaO) was observed. The emergence of this new phase occurred through the incorporation of the solvent into the HAp matrix.

SEM images showed preservation of surface topology and microstructure, suggesting that the incorporation protocol maintained the physical integrity of HA, which is advantageous for biomaterial applications, as stable surfaces tend to retain osteoconductive properties and favorable cell interactions. This observation is consistent with reports that drug functionalization of bioceramics often does not alter the primary crystalline phase, mainly when incorporation occurs by surface adsorption or into amorphous regions. (Ishack S. et al., 2017; Wang M.M. et al., 2019)

EDS analysis identified the expected HA-related elements (Ca, P, O, C) and did not detect nitrogen, which would be indicative of DIPY (the drug contains nitrogen atoms). This absence aligns with known limitations of EDS: the technique has low sensitivity for light elements (e.g., N) and for small amounts or inhomogeneous surface distributions of organic compounds. Therefore, complementary techniques are sensitive to functional groups. (Todd E.A. et al., 2024)

4 Conclusion

The present study evaluated the incorporation of DIPY into HAp synthesized via wet precipitation, using different methods and solvents. SEM analyses showed no significant changes in the surface morphology of the samples, regardless of solvent type, DIPY concentration, or incorporation method, indicating the material's structural stability.

EDS results revealed the predominant presence of elements characteristic of HA (C, O, and Ca). However, nitrogen, a component of the DIPY structure, was not detected. This absence may be attributed to the technique's low sensitivity to light elements or to an insufficient amount of incorporated drug, highlighting the need for more sensitive analytical methods, such as FTIR or Raman spectroscopy, to confirm the presence of DIPY.

XRD analyses revealed a partial phase transformation of hydroxyapatite (HAp), with the emergence of calcium oxide (CaO) ($\approx 2\theta 42^\circ$, indexed to ICCD 01-072-1243), while the remaining reflections were consistent with HAp (ICCD 00-054-0022). This change was observed for both immersion and dropwise application protocols. Nevertheless, based on the techniques applied in this study, effective DIPY incorporation could not be confirmed.

Despite these limitations, the results reinforce the potential of hydroxyapatite as a biomaterial for drug functionalization with osteogenic interest. Future studies should include complementary chemical characterization methods and both in vitro and in vivo biological assays to elucidate the efficiency of DIPY incorporation and its osteoinductive performance, to develop advanced bioceramics for bone regeneration applications.

References

1. Ali, A., et al. (2019). *Dipyridamole enhances bone regeneration through adenosine receptor signaling pathways*. *Frontiers in Pharmacology*, 10, 137.
2. Dorozhkin, S. V. (2010). *Bioceramics of calcium orthophosphates*. *Biomaterials*, 31(7), 1465–1485.
3. LeGeros, R. Z. (2008). *Calcium phosphate-based osteoinductive materials*. *Chemical Reviews*, 108(11), 4742–4753.
4. Rezwani, K., et al. (2006). *Biodegradable and bioactive porous polymer/inorganic composite scaffolds for bone tissue engineering*. *Biomaterials*, 27(18), 3413–3431.
5. Yao, Y., et al. (2020). *Dipyridamole promotes bone healing by enhancing angiogenesis and osteogenesis*. *Biomedicine & Pharmacotherapy*, 127, 110203.
6. SILVEIRA, P. H. P. M. d.; LOPES, I. J. V. R.; RIBEIRO, S. B. N. et al. Synthesis and characterization of lithium fluoride-doped hydroxyapatite by aqueous precipitation. *Contribuciones a las Ciencias Sociales*, v. 17, n. 7, p. e8293, 2024. Disponível em: <<https://doi.org/10.55905/revconv.17n.7-141>>.
7. Ishack S., Mediero A., Wilder T., Ricci J.L., Cronstein B. N. Bone regeneration in critical bone defects using three-dimensionally printed β -tricalcium phosphate/hydroxyapatite scaffolds is enhanced by coating scaffolds with either dipyridamole or BMP-2. *J Biomed Mater Res B Appl Biomater*. 2017.
8. Wang M. M., et al. Dipyridamole-loaded 3D-printed bioceramic scaffolds: (Nature Scientific Reports, 2019) - study of DIPY-3DPBC scaffolds and bone regeneration.

9. Bekisz J. M., et al. Dipyridamole enhances osteogenesis of three-dimensional printed bioceramic scaffolds. (2017/2018) - work supporting DIPY's pro-osteogenic effects in scaffolds.
10. Todd E.A., et al. Functional Scaffolds for Bone Tissue Regeneration — review on scaffold functionalization and analytical/biological evaluation strategies (MDPI, 2024).
11. Kumar A., et al. Additive Manufacturing Methods for Producing Bioceramic Scaffolds — discusses the incorporation of bioactive agents like DIPY into HAp/ β -TCP constructs.
12. National Institute of Standards and Technology. NIST Chemistry WebBook: Ethanol - Thermophysical Properties. Gaithersburg (MD): NIST; 2024. Available from: <https://webbook.nist.gov/cgi/cbook.cgi?ID=C64175&Units=SI>
13. National Institute of Standards and Technology. NIST Chemistry WebBook: Methanol - Thermophysical Properties. Gaithersburg (MD): NIST; 2024. Available from: <https://webbook.nist.gov/cgi/cbook.cgi?ID=C67561&Units=SI>
14. PubChem. Ethanol [Internet]. Bethesda (MD): National Library of Medicine; 2024 [cited 2025 Sep 19]. Available from: <https://pubchem.ncbi.nlm.nih.gov/compound/Ethanol>
15. PubChem. Methanol [Internet]. Bethesda (MD): National Library of Medicine; 2024 [cited 2025 Sep 19]. Available from: <https://pubchem.ncbi.nlm.nih.gov/compound/Methanol>
16. Bozorgmehr B, Farhadi S, Nazari F, Vafaei S. Numerical simulation of evaporation of ethanol–water droplets. *ACS Omega*. 2021;6(19):12910-8. doi:10.1021/acsomega.1c00613
17. McGlashan ML, Potter HL. Isothermal liquid-vapor equilibria for the system methanol-water. *J Chem Eng Data*. 1976;21(2):196-8. doi:10.1021/je60069a012
18. Kurihara K, Takeda K, Kojima K. Isobaric vapor–liquid equilibria for methanol + ethanol + water and constituent binaries. *Fluid Phase Equilibria*. 1993;85:1-14. doi:10.1016/0378-3812(93)85067-Q
19. Dortmund Data Bank. VLE data for ethanol-water and methanol-water systems [Internet]. Dortmund: DDBST GmbH; 2024 [cited 2025 Sep 19]. Available from: <https://www.ddbst.com/en/EED/VLE/VLE.html>